

Cationic long-chain ceramide LCL-30 induces cell death by mitochondrial targeting in SW403 cells

Daniel Dindo,¹ Felix Dahm,¹ Zdzislaw Szulc,²
Alicja Bielawska,² Lina M. Obeid,^{2,3}
Yusuf A. Hannun,² Rolf Graf,¹
and Pierre-Alain Clavien¹

¹Swiss HPB (Hepato-Pancreato-Biliary) Center, Department of Visceral and Transplantation Surgery, University Hospital Zurich, Zurich, Switzerland; ²Department of Biochemistry and Molecular Biology, Medical University of South Carolina, Charleston, South Carolina; and ³Research Service, Department of Veterans Affairs Medical Center, Charleston, South Carolina

Abstract

Ceramides are sphingolipid second messengers that are involved in the mediation of cell death. There is accumulating evidence that mitochondria play a central role in ceramide-derived toxicity. We designed a novel cationic long-chain ceramide [ω -pyridinium bromide D-*erythro*-C₁₆-ceramide (LCL-30)] targeting negatively charged mitochondria. Our results show that LCL-30 is highly cytotoxic to SW403 cells (and other cancer cell lines) and preferentially accumulates in mitochondria, resulting in a decrease of the mitochondrial membrane potential, release of mitochondrial cytochrome *c*, and activation of caspase-3 and caspase-9. Ultrastructural analyses support the concept of mitochondrial selectivity. Interestingly, levels of endogenous mitochondrial C₁₆-ceramide decreased by more than half, whereas levels of sphingosine-1-phosphate increased dramatically and selectively in mitochondria after administration of LCL-30, suggesting the presence of a mitochondrial sphingosine kinase. Of note, intracellular long-chain ceramide levels and sphingosine-1-phosphate remained unaffected in the cytosolic and extramitochondrial (nuclei/cellular membranes) cellular fractions. Furthermore, a synergistic effect of cotreatment of LCL-30 and doxorubicin was observed, which was not related to alterations in endogenous ceramide levels.

Received 12/12/05; revised 4/5/06; accepted 4/21/06.

Grant support: Novartis Foundation-Switzerland, Hartmann-Muller Foundation-Switzerland, and EMDO Foundation-Switzerland (D. Dindo), SNF grant 109906 (P.-A. Clavien) and NIH grants CA97132 (Y.A. Hannun) and AG16583 (L.M. Obeid).

The costs of publication of this article were defrayed in part by the payment of page charges. This article must therefore be hereby marked advertisement in accordance with 18 U.S.C. Section 1734 solely to indicate this fact.

Note: D. Dindo and F. Dahm contributed equally to this work.

Requests for reprints: Pierre-Alain Clavien, Department of Visceral and Transplantation Surgery, University Hospital Zurich, Rämistrasse 100, CH-8091 Zurich, Switzerland. Phone: 41-1-255-33-00; Fax: 41-1-255-44-49. E-mail: clavien@chir.unizh.ch

Copyright © 2006 American Association for Cancer Research.

doi:10.1158/1535-7163.MCT-05-0513

Cationic long-chain pyridinium ceramides might be promising new drugs for cancer therapy through their mitochondrial preference. [Mol Cancer Ther 2006;5(6):1520–9]

Introduction

Ceramides have emerged as important lipid second messengers involved in cell growth, differentiation, senescence, and death (1). The intracellular levels of this sphingolipid are elevated in tumor cells after irradiation or therapy with anticancer drugs, such as doxorubicin (2), implicating endogenous ceramides as important mediators of cancer therapy (3). It has also been shown that exogenous ceramides induce cell death in a variety of human cancer cell types (4). Interestingly, cancer cells seem to be more susceptible to the toxic effect of exogenous ceramides than normal cells (5–7), rendering exogenous ceramides promising novel drugs for chemotherapy.

There is accumulating evidence that mitochondria play a central role in ceramide-derived cell death. Studies on isolated mitochondria revealed that ceramides released cytochrome *c* from mitochondria (8–10), and ceramide was reported to activate a mitochondrial protein phosphatase 2A, which dephosphorylates the antiapoptotic Bcl-2 molecule and leads to cell death (11). Furthermore, indirect modification of Bcl-2 by ceramide was also reported by targeting the nonmitochondrial cathepsin D (12). Targeting of sphingomyelinase to mitochondria, but not other subcellular compartments, resulted in translocation of Bax and activation of the mitochondrial pathway of apoptosis (13). Moreover, ceramide-metabolizing enzymes have also been detected in mitochondria, and these include neutral/alkaline ceramidase (14) and ceramide synthase (15). Functionally, ceramide was shown to block mitochondrial respiratory chain complex I/III by a direct interaction (9, 16); finally, ceramide has been shown to induce the production of reactive oxygen species (ROS) in intact mitochondria (8).

Mitochondria from cancer cells and from normal cells differ in many aspects, offering mitochondria as potential targets for cancer therapy. First, the metabolism of cancer cells is characterized by an increased anaerobic glycolysis that is not influenced by the oxygen concentration rendering cancer cells resistant to hypoxia (Warburg effect). Secondly, differences in the permeability transition pore complex from cancer versus normal cells have been repeatedly described (17–19). Furthermore, the mitochondrial membrane potential ($\Delta\psi_m$) is higher in cancer compared with normal cells (20).

Cationic lipophilic molecules accumulate within the mitochondrial matrix driven by the electrochemical gradient, which could favor increased accumulation in mitochondria of cancer cells. Positively charged short-chain (C₆) ceramides were shown to be enriched in mitochondria and to induce cell death (10). Because naturally occurring

ceramides have an acyl chain of ≥ 14 carbon atoms, we designed a novel cationic ω -pyridinium bromide *D-erythro*-C₁₆-ceramide (LCL-30) and investigated (a) its toxicity, (b) its intracellular distribution, and (c) the influence of this long-chain ceramide on endogenous ceramide levels in SW403 human colon cancer cells. As doxorubicin is also a cationic lipophilic molecule and has been shown to exert at least some of its toxicity by interference with the endogenous ceramide levels, we tested the combined effects of LCL-30 with doxorubicin.

Materials and Methods

Synthesis and Solubilization of the Ceramide Analogue LCL-30

Cationic LCL-30 was synthesized in the Medical University of South Carolina Lipidomics Core.⁴ For experimental use, LCL-30 was dissolved in ethanol to 10 mmol/L stock solutions and kept at -20°C .

Cell Culture and Biological Reagents

SW403 human colon carcinoma cells (CCL-230; American Type Culture Collection, Manassas, VA) were cultured in DMEM (Life Technologies, Carlsbad, CA) supplemented with 10% fetal bovine serum (PAA Laboratories GmbH, Cölbe, Germany) and 100 units/mL penicillin and 100 $\mu\text{g}/\text{mL}$ streptomycin (Life Technologies). The cells were maintained at 37°C in a 5% CO_2 atmosphere.

C₂- and C₆-ceramides were purchased from Avanti Polar Lipids (Alabaster, AL). C₁₆-ceramide, actinomycin D, rotenone, *N*-acetylcysteine, and cyclosporine A were from Sigma (St. Louis, MO). Recombinant human tumor necrosis factor- α was purchased from R&D Systems (Minneapolis, MN). Caspase-3 and caspase-9 substrates (Ac-DEVD-AFC and Ac-LEHD-AFC, respectively) as well as pan-caspase inhibitor (Z-VAD-FMK) were from Alexis Biochemicals (Lausen, Switzerland). Doxorubicin HCl (Sigma) was dissolved in 0.9% NaCl and kept at 4°C .

Cell Viability Assay

Cells were seeded into 12-well plates at a density of $\sim 50\%$ corresponding to 0.5×10^6 per well, left to adhere overnight, and subjected to the specified conditions for a period of 12 or 24 hours. Then, medium was changed and the number of viable cells was assessed by the addition of 40 μL of a 0.5% tetrazolium salt solution [3-(4,5-dimethylthiazol-2-yl)-2,5-diphenyltetrazolium bromide (MTT); Sigma]. After 60 minutes of incubation, the formation of the formazan product was monitored by measuring absorbance at 570 nm after solubilization in acidic isopropanol (5% formic acid in isopropanol). Values were calculated as percentage of untreated controls. In all conditions, cells were exposed to ethanol in a nontoxic concentration of 0.05% (v/v). In parallel, cells were incubated as described above. Cells were then detached using 1% trypsin and centrifuged at $800 \times g$. Cell pellets were resuspended in PBS, and trypan blue (Sigma) staining was assessed by light microscopy.

Caspase-3/Caspase-9 Activity

SW403 cells were cultured under the specified conditions, and caspase activity was measured after 12 hours of incubation. Adherent cells were scraped and lysed [10 mmol/L Tris-HCl (pH 7.4), 2 mmol/L EDTA, 0.1% NP40] for 10 minutes at 4°C . After centrifugation for 10 minutes at $10,000 \times g$, protein concentration was measured using the Bio-Rad detergent-compatible protein assay (Bio-Rad Laboratories, Hercules, CA). Lysate corresponding to 25 μg protein was incubated for 30 minutes at room temperature with or without 1 $\mu\text{mol}/\text{L}$ pan-caspase inhibitor Z-DEVD-FMK. Then, caspase-3 substrate Ac-DEVD-AFC (10 $\mu\text{mol}/\text{L}$) or caspase-9 substrate Ac-LEHD-AFC (10 $\mu\text{mol}/\text{L}$), and DTT (10 mmol/L final concentration) were added, and enzyme activity was monitored by measuring fluorescence at $390_{\text{ex}}/538_{\text{em}}$ nm (Biolise software, Fluostar SLT-Lab Instruments, Crailsheim, Germany). Caspase activity was then calculated by determining the relative fluorescence units generated under steady-state kinetics from which values of caspase-independent protease activity in the presence of the corresponding inhibitor were subtracted.

Terminal Deoxynucleotidyl Transferase – Mediated dUTP Nick End Labeling Staining

SW403 cells were cultured under the specified conditions, trypsinized, and resuspended in culture medium ($1 \times 10^6/\text{mL}$). An aliquot (100 μL) of the cell suspension was centrifuged in a Shendon Cytospin III at 500 rpm for 2 minutes (ThermoShendon, Pittsburgh, PA). Slides were air-dried for 30 minutes and then stored at -80°C . Slides were thawed at room temperature, washed with PBS, and placed in methanol/ H_2O_2 (2%) for 8 minutes. After washing with PBS, cells were permeabilized with Tri-X buffer (0.1% Triton X, 0.1% sodium citrate in H_2O) for 2 minutes on ice, washed again with PBS, stained with terminal deoxynucleotidyl transferase-mediated dUTP nick end labeling reaction mixture (*In situ* Cell Death Detection kit, Roche Diagnostics GmbH, Mannheim, Germany), and incubated for 30 minutes at 60°C .

Measurement of Intracellular Doxorubicin Concentration

For determination of cellular doxorubicin uptake, cells were trypsinized and washed with ice-cold PBS. The pellet was resuspended with 100 μL ice-cold PBS and then mixed for 30 seconds with 500 μL chloroform/methanol (4:1, v/v). After centrifugation with $1,200 \times g$ for 15 minutes, 100 μL of the organic phase were removed and endogenous fluorescence of doxorubicin was measured in a fluorescence spectrophotometer $470_{\text{ex}}/585_{\text{em}}$ nm (Fluostar).

Determination of $\Delta\psi_m$

SW403 cells were maintained in flasks (25 cm^2) and cultured at the specified conditions. Cells were then washed in PBS, and fresh cell medium supplemented with MitoTracker (Molecular Probes, Inc., Eugene, OR) was added according to the manufacturer's instructions. After 30 minutes, cells were washed in PBS and trypsinized. After resuspension in PBS, cells were analyzed by flow cytometry (FACSCalibur, Becton Dickinson, Franklin Lakes, NJ).

⁴ Z. Szulc and A. Bielawska, in preparation.

Western Blot Analysis for Cytochrome *c*

For analysis of cytochrome *c* release, cells were trypsinized and washed with ice-cold PBS. Mitochondrial and cytosolic (S100) fractions were prepared from cells suspended in 50 μ L ice-cold buffer containing 20 mmol/L HEPES-KOH (pH 7.5), 10 mmol/L KCl, 1.5 mmol/L MgCl₂, 1 mmol/L sodium EDTA, 1 mmol/L DTT, 0.1 mmol/L phenylmethylsulfonyl fluoride, and 250 mmol/L sucrose. Mechanical homogenization was achieved by repeated aspiration through a pipette. Cells and nuclei that were not lysed were pelleted by 10 minutes of centrifugation (750 \times *g*, 4°C). The supernatant was centrifuged at 10,000 \times *g* for 15 minutes at 4°C. The resulting pellet, representing the mitochondrial fraction, was then resuspended in 10 μ L of the buffer described above. Finally, the supernatant was centrifuged at 100,000 \times *g* for 1 hour at 4°C. Both fractions were stored at -80°C until used. Mitochondrial and cytosolic fractions were diluted in sample buffer [187.5 mmol/L Tris-HCl (pH 6.8), 6% SDS, 30% glycerol, 150 mmol/L DTT, 0.3% bromophenol blue] and then boiled for 10 minutes at 90°C. Samples were run on 16% Novex Tris-glycine gel (Life Technologies), blotted onto polyvinylidene difluoride membrane, and incubated with a mouse anti-cytochrome *c* monoclonal antibody (PharMingen, San Diego, CA).

Glutathione Determination

Cells were cultured in 25-cm² flasks and treated with the indicated substances. After washing with PBS, intracellular glutathione (GSH) levels were determined with a GSH kit (Oncogene, San Diego, CA) according to the manufacturer's instructions.

Transmission Electron Microscopy

SW403 cells were prefixed with 1.5% glutaraldehyde and 0.8% paraformaldehyde (0.1 mol/L cacodylate buffer) for 30 minutes at room temperature and postfixed in an aqueous solution of 1% OsO₄ + 1.5% K₄(FeCN)₆ for 1 hour. The specimens were then embedded into Epon by routine procedure. Semithin sections (~1 μ m) were stained with toluidine blue and analyzed by light microscopy. Ultrathin sections (~50 nm) were contrasted with lead citrate and uranyl acetate and studied with a Philips CM100 transmission electron microscope (Zurich, Switzerland).

Analysis of Endogenous Ceramide Species by Liquid Chromatography-Mass Spectrometry

Electrospray ionization-tandem mass spectrometry analysis of endogenous ceramide species was done in the Medical University of South Carolina Lipidomics Core on a Thermo Finnigan (Waltham, MA) TSQ 7000 triple quadrupole mass spectrometer, operating in a multiple reaction monitoring-positive ionization mode. Briefly, cell pellets corresponding to ~2 \times 10⁶ to 3 \times 10⁶ cells were fortified with the internal standards and lipids were extracted and analyzed as described.⁵

⁵ J. Bielawski, Z.M. Szulc, Y.A. Hannun, and A. Bielawska. Methods. In press 2005.

Statistical Analysis

Data are mean \pm SD of *n* independent experiments. Mann-Whitney *U* test and one-way ANOVA were used where appropriate. *P* < 0.05 was considered statistically significant.

Results

Is Cationic LCL-30 Toxic to Cancer Cells?

The first set of experiments was to determine cytotoxicity of the novel cationic long-chain ceramides. SW403 cells were cultured in the presence of LCL-30 at concentrations of 1 to 5 μ mol/L for 12 and 24 hours. Cell viability was assessed by the MTT assay (Fig. 1A). Cell viability decreased in a concentration- and time-dependent manner. The IC₅₀ for LCL-30 was 5.2 \pm 1.5 μ mol/L. For comparison, conventional *D-erythro-C*₂, -*C*₆, and -*C*₁₆-ceramides did not induce cell death when used at the same concentrations as LCL-30 (Fig. 1A). After 48 hours of LCL-30 treatment (5 μ mol/L), cell viability decreased to 14 \pm 5% (Fig. 1B). To exclude the possibility that the mitochondrial dehydrogenases were selectively inhibited without affecting cell viability or that the MTT results were confounded by differences in cell

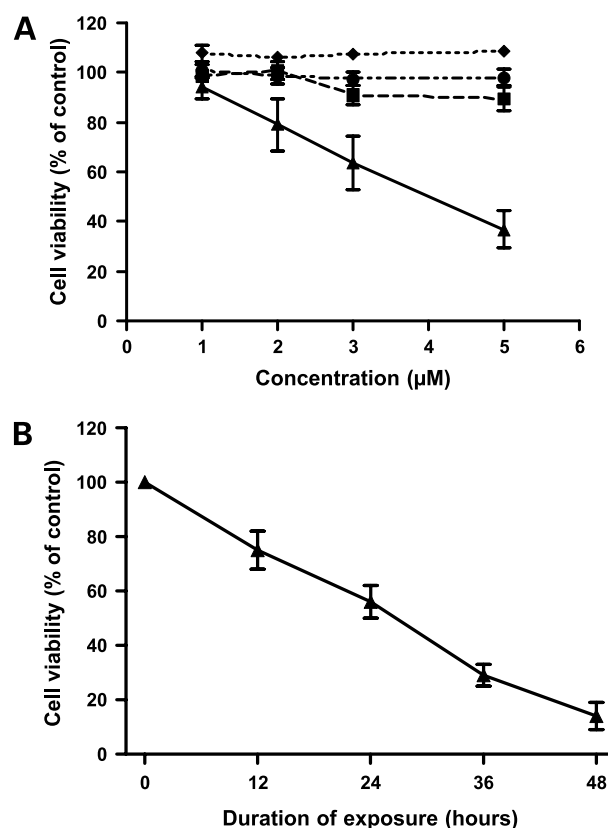


Figure 1. **A**, cell viability was assessed by MTT assay in SW403 cells incubated at the indicated concentrations for 24 h. *C*₂, *C*₆, and *C*₁₆-ceramides did not have any effect on cell viability in SW403 cells. **B**, SW403 cells were treated with LCL-30 (5 μ mol/L). Cell viability was assessed by MTT at the indicated time points. Points, mean of three independent experiments; bars, SD. ♦, *C*₂-ceramide; ■, *C*₆-ceramide; ●, *C*₁₆-ceramide; ▲, LCL-30.

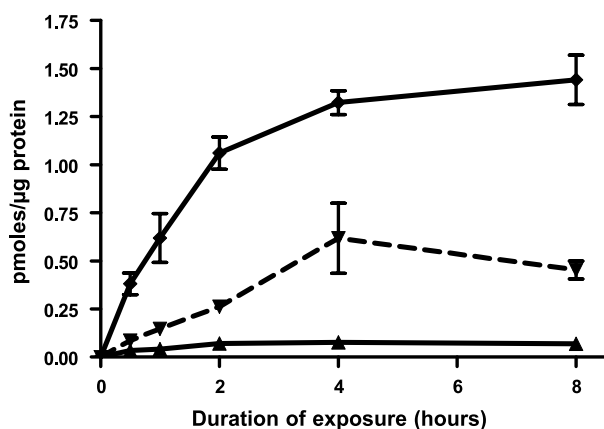


Figure 2. LCL-30 uptake was measured by mass spectrometry. LCL-30 concentration was analyzed in three different cellular fractions: mitochondria, cytosol, and the extramitochondrial fractions mainly constituting the nucleus and cellular membranes. Points, mean of three independent experiments; bars, SD. ♦, mitochondria; ▲, cytosol; ▼, extramitochondrial.

growth, we also tested cell viability by trypan blue exclusion. These results supported the findings of the MTT assay (data not shown). Similar findings by MTT and trypan blue exclusion test were obtained in the colon cancer cell lines LoVo and CT26 and in the human hepatoma cell lines HepG2, Hep3B, and HuH7 (data not shown). Interestingly, no toxicity of LCL-30 could be observed in freshly isolated rat hepatocytes. Cytotoxicity was also evaluated by terminal deoxynucleotidyl transferase-mediated dUTP nick end labeling assay identifying nuclear DNA fragmentation from which the results underscore the toxic effect of LCL-30 (see below). For further analyses, we concentrated on the human colon cancer cell line SW403 because previous work by our group was also done in this cell line (7).

Does Cationic LCL-30 Preferentially Accumulate in Mitochondria?

Mitochondria of SW403 cells that had been incubated with LCL-30 (5 $\mu\text{mol/L}$) for 0.5, 1, 2, 4, and 8 hours were isolated. The cytosolic fraction and the extramitochondrial cellular fraction were also used for liquid chromatography-mass spectrometry analysis. In the cytosolic fraction, no increase of LCL-30 could be detected. LCL-30 preferentially accumulated in the mitochondria and, to a much lesser extent, in the extramitochondrial fraction, mainly constituting cellular membranes and nuclei (Fig. 2). After 8 hours of treatment, LCL-30 concentration in mitochondria reached 1.4 pmol/ μg protein, whereas in the extramitochondrial fraction it was at 0.6 pmol/ μg protein. Twenty percent of the total LCL-30 per sample was detectable within the mitochondrial fraction (1,250 versus 6,300 pmol/sample). The difference in volume of these two fractions further underscores the relative selectivity of LCL-30 accumulation within mitochondria.

Does Cationic LCL-30 Exert Mitochondrial Toxic Effects?

Breakdown of $\Delta\psi_m$ and cytochrome *c* release was suggested as the primary pathway mediating cell death

in ceramide-treated cells (21). The disruption of $\Delta\psi_m$ has been identified as point-of-no-return of cell death because respiration is blocked as soon as $\Delta\psi_m$ decreases and cytochrome *c* is released.

In our study, $\Delta\psi_m$ was determined by the fluorochrome CMXRos in SW403 cells treated with the cationic ceramide LCL-30 (5 $\mu\text{mol/L}$). A drop in $\Delta\psi_m$ was observed by flow cytometry in LCL-30-treated cells as early as after 4 hours of treatment (Fig. 3A), which was accompanied by mitochondrial release of cytochrome *c* into the cytosol (Fig. 3B). For the latter analysis, doxorubicin served as positive control.

The decrease of $\Delta\psi_m$ may be related to the opening of mitochondrial membrane permeability transition pores, which can be inhibited by cyclosporin A (22). In our study, cyclosporin A (1 $\mu\text{mol/L}$) did not maintain $\Delta\psi_m$, suggesting that mitochondrial transition pores were not involved in LCL-30-induced breakdown of $\Delta\psi_m$ (Fig. 3A). Cyclosporin A-insensitive mechanisms for ceramide-induced collapse of $\Delta\psi_m$ have been postulated by others (9, 23, 24).

Ceramide may induce oxidative damage by ROS generation of mitochondria (25) or by inhibiting the ROS

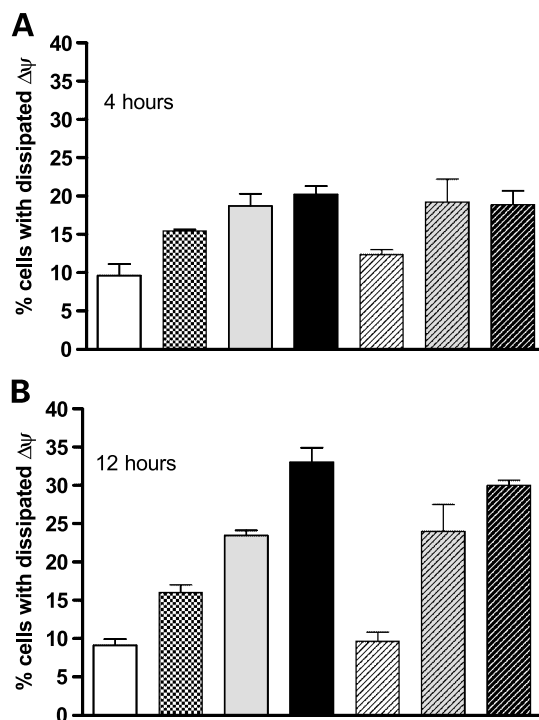


Figure 3. A, $\Delta\psi_m$ was determined by the fluorochrome CMXRos (flow cytometry) in SW403 cells treated with the cationic ceramide LCL-30. For this experiment, cells were exposed to the specific condition for 4 and 12 h. White columns, control; checkered columns, doxorubicin (1 $\mu\text{mol/L}$); gray columns, LCL-30 (5 $\mu\text{mol/L}$); black columns, LCL-30/doxorubicin; striped columns, addition of cyclosporin A to specific condition (1 $\mu\text{mol/L}$). B, representative Western blot of cytochrome *c* release from mitochondria (M) into the cytosol (C) after 24 h of incubation with doxorubicin (Dox; 1 $\mu\text{mol/L}$) and LCL-30 (5 $\mu\text{mol/L}$).

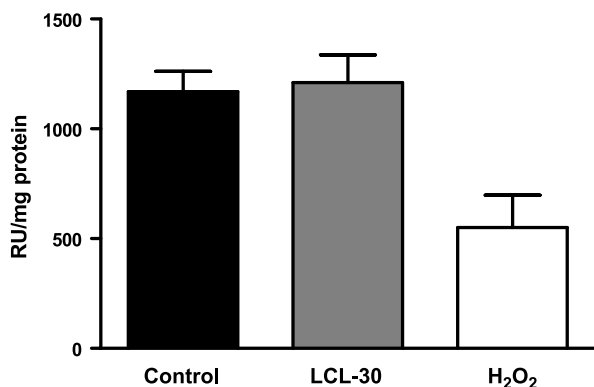


Figure 4. SW403 cells were incubated for 12 h with LCL-30 (5 $\mu\text{mol/L}$) and intracellular GSH levels were determined. H₂O₂ (100 mmol/L) for 2 h served as positive control. Columns, mean relative units (RU)/mg protein of three experiments; bars, SD.

scavenger GSH (8), although conflicting data have been reported (26–28). We determined intracellular GSH levels after treatment of SW403 cells with LCL-30 (Fig. 4). After 12 hours of treatment, no decrease in GSH was observed. To support this finding, cells were pretreated with the selective complex I inhibitor rotenone (5 $\mu\text{mol/L}$), which

blocks ROS generation from mitochondria (29), and *N*-acetylcysteine (100 $\mu\text{mol/L}$), a reducing agent and a precursor of GSH. Rotenone and *N*-acetylcysteine did not improve cell survival as assessed by MTT assay, supporting that mitochondrial ROS are not involved in cationic long-chain ceramide toxicity (data not shown).

Cellular morphology has been used as a criterion to discriminate apoptotic from necrotic cell death. Although biochemical markers indicated an apoptotic form of programmed cell death in our study, transmission electron microscopy was used to further elucidate the type of cell death. Mitochondria, endoplasmic reticulum, nuclear membrane, and chromatin were examined after 4, 12, and 24 hours of treatment. Untreated SW403 cells were characterized by large nuclei and were rich in mitochondria and lipid droplets. After incubation with cationic ceramide, morphology changed significantly, showing cell swelling with loss of microvilli and nuclei with condensed chromatin (Fig. 5), although these nuclear alterations did not include any fragmentation of the nucleus. These data are in line with other studies (30, 31), showing only slight nuclear changes in ceramide-treated cells. However, mitochondria were markedly swollen with increase in mitochondrial matrix volume and unfolded cristae (Fig. 5). The inner membrane was apparently intact, whereas the outer

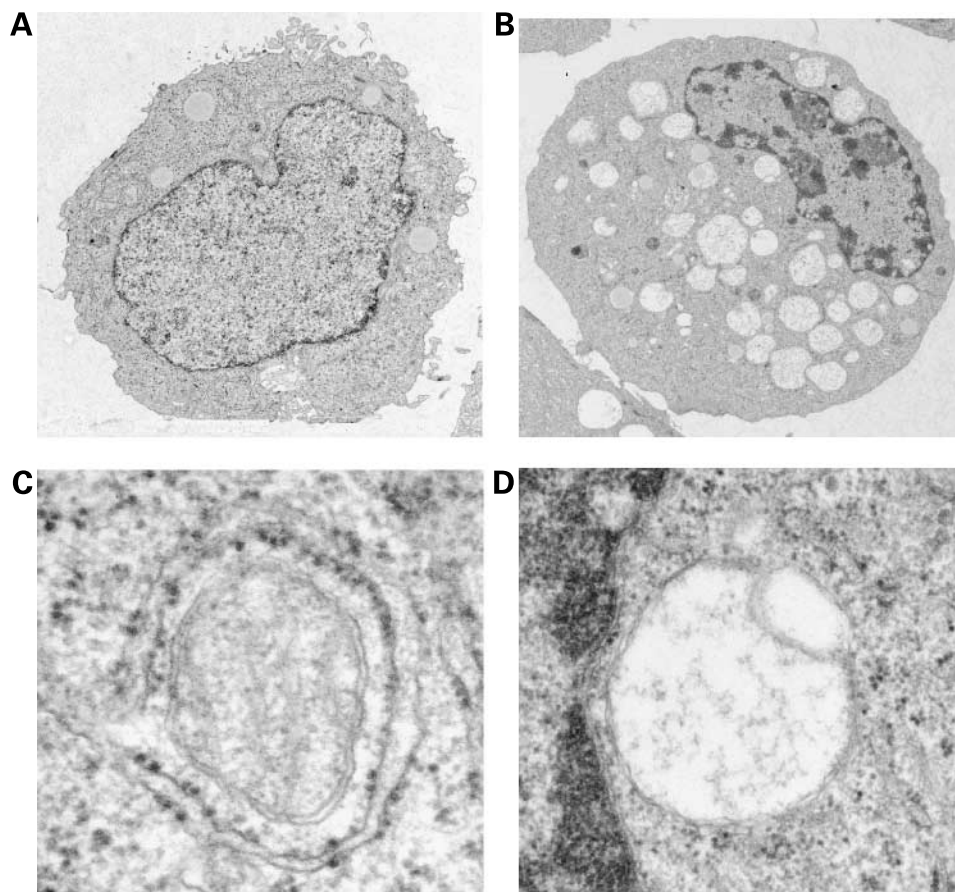


Figure 5. Transmission electron microscopy of SW403 cells. Magnification, $\times 7,100$. Cells were incubated for 24 h with LCL-30. **A**, control; **B**, LCL-30 (5 $\mu\text{mol/L}$). Treatment with LCL-30 resulted in marked "vacuolization" of the cytoplasm. These vacuoles represented swollen mitochondria identified by their double-layer membrane. The nucleus contained dense chromatin, whereas nuclear fragmentation was absent, although the nucleus was highly lobulated. Magnification, $\times 44,000$. **C**, control; **D**, LCL-30 (5 $\mu\text{mol/L}$). After LCL-30 treatment, mitochondria were highly distended with destruction of the inner mitochondrial matrix. Outer mitochondrial membrane was disrupted in many mitochondria. Of note, nuclear membrane was intact, although mitochondria were highly destroyed (**D**).

membrane seemed to be ruptured in most of the mitochondria. These changes were already apparent after 4 hours of treatment. Of note, after 24 hours of treatment, nuclear and plasma membranes were still preserved in most of the cells despite the destruction of most of the mitochondria. No membrane blebbing could be observed. Moreover, the endoplasmic reticulum was not enlarged, and ribosomes of the rough endoplasmic reticulum were not detached. This is in contrast to a study showing alterations of endoplasmic reticulum to be the first sign in C₂-ceramide-treated PC12 cells (30). Thus, ultrastructural morphology suggests mitochondria to be the primary target of cationic LCL-30 in SW403 cells.

Does Cationic LCL-30 Affect Endogenous Ceramide Levels?

Endogenous ceramide levels were studied after treatment of SW403 cells with LCL-30 (5 μmol/L) at various time points. The cytosolic, mitochondrial, and extramitochondrial (nuclei and cellular membranes) fractions were analyzed. No change of total ceramide levels was found within 8 hours of treatment in the cytosolic and extramitochondrial fractions. These findings were also obtained from analyses of C₁₄, C₁₆, C₁₈, C_{18:1}, C₂₀, C₂₄, and C_{24:1} levels. However, total endogenous ceramide levels decreased in the mitochondrial fraction in a time-dependent manner (Fig. 6A). This decrease was accounted for by a selective drop of mitochondrial C₁₆-ceramide because the levels of C₁₄, C₁₈, C_{18:1}, C₂₀, C₂₄, and C_{24:1}-ceramide in mitochondria remained unaffected. C₁₆-ceramide is the most abundant ceramide in many cell types as it is in SW403 cells: C₁₆-ceramide constituted almost half of the total endogenous ceramide concentration. Importantly, the total of mitochondrial C₁₆-ceramides representing endogenous C₁₆-ceramide and the exogenous cationic LCL-30 increased over time (Fig. 6B).

We also determined endogenous levels of the ceramide metabolites sphingosine and sphingosine-1-phosphate (S1P). Sphingosine may occur in the early stage of apoptosis and may also represent a mediator of cell death. Sphingosine can be phosphorylated by sphingosine kinases to form S1P, which has antiapoptotic properties and may antagonize ceramide-mediated cell death (32). Endogenous levels of sphingosine remained unaffected by LCL-30 in all of the cellular fractions. In contrast, S1P significantly increased over time in the mitochondrial but not in the cytosolic and extramitochondrial fractions (Fig. 6C). In untreated cells, S1P was below detection limits in all fractions analyzed.

Does the Coadministration of Doxorubicin Enhance Cell Toxicity of Cationic LCL-30?

Doxorubicin is a commonly used chemotherapeutic agent from the family of the anthracyclines. Like LCL-30, doxorubicin is a lipophilic cationic molecule that may compromise mitochondrial integrity (33). There is strong evidence that doxorubicin increases endogenous ceramide levels in cancer cells by either activation of neutral sphingomyelinase and/or induction of the *de novo* pathway of ceramide metabolism (2, 34–38). The IC₅₀ of doxorubicin in the SW403 cell line was 2.5 ± 0.3 μmol/L. When

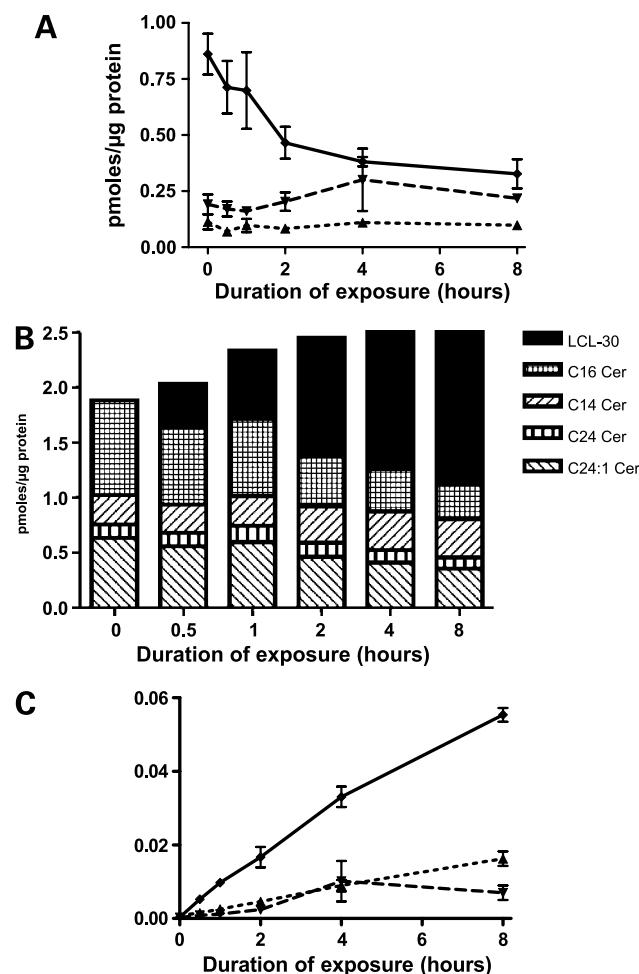


Figure 6. A, SW403 cells were treated with LCL-30 (5 μmol/L) for the indicated time. Mass spectrometry analyses of C₁₆-ceramide levels were done for the mitochondrial, cytosolic, and extramitochondrial cellular fractions. Points, mean of three experiments; bars, SD. ♦, mitochondria; ▲, cytosol; ▼, extramitochondrial. B, SW403 cells were treated with LCL-30 (5 μmol/L) for the indicated time. Mass spectrometry analyses of total endogenous ceramide and the LCL-30 levels were done for the mitochondrial fraction. Regarding endogenous ceramide levels, data are shown for the most abundant ceramide species C₁₄, C₁₆, C₂₄, and C_{24:1} in SW403 cells. C, SW403 cells were treated with LCL-30 (5 μmol/L) for the indicated time. S1P levels were measured for the mitochondrial, cytosolic, and extramitochondrial cellular fractions by mass spectrometry. Points, mean of three experiments; bars, SD. ♦, mitochondria; ▲, cytosol; ▼, extramitochondrial.

doxorubicin was added in a 1 μmol/L concentration to 5 μmol/L LCL-30, the response was enhanced. Survival decreased from 57.3 ± 8.8% to 35.6 ± 0.8% within 24 hours of treatment as assessed by MTT assay (Fig. 7A). To differentiate whether enhanced cell death in response to LCL-30 in combination with doxorubicin was additive or synergistic, we employed the fractional product method [$fu(1,2) = fu(1) \times fu(2)$; ref. 31]. At a concentration of 1 μmol/L doxorubicin and 5 μmol/L LCL-30, an additive effect would predict a viability of ≥54.4%. The results, however, showed a combined effect of <54.4%, suggesting

a synergistic effect between doxorubicin and LCL-30 (Fig. 7B). This synergistic effect was also reflected by results of caspase-3 and caspase-9 (Fig. 7C) and the terminal deoxynucleotidyl transferase-mediated dUTP nick end labeling assays (Fig. 7D).

To test the possibility that the novel cationic long-chain ceramide facilitated doxorubicin uptake, intracellular doxorubicin concentrations were measured at various time points (0.5, 1, 2, and 3 hours). Doxorubicin uptake was not altered by the addition of LCL-30 within this time period. Surprisingly, doxorubicin did not affect endogenous ceramide levels in SW403, either. Levels of C₁₄-C₂₄ and levels of the ceramide metabolites sphingosine and S1P remained unchanged in all the three fractions analyzed.

Discussion

In this study, we developed a novel long-chain ceramide analogue and showed that it is highly cytotoxic to cancer cells by mitochondrial targeting. The cationic pyridinium C₁₆-ceramide LCL-30 preferentially accumulated in mitochondria, resulting in breakdown of $\Delta\psi_m$, release of the proapoptotic cytochrome *c*, and activation of caspase-9 and caspase-3. Endogenous mitochondrial ceramide levels decreased after treatment with LCL-30, whereas the ceramide levels remained unaltered in the extramitochondrial and cytosolic fractions. S1P, which is known to have antiapoptotic properties, dramatically increased exclusively within mitochondria. Furthermore, this ceramide analogue acted synergistically with doxorubicin in the induction of cell death. This effect was not related to an

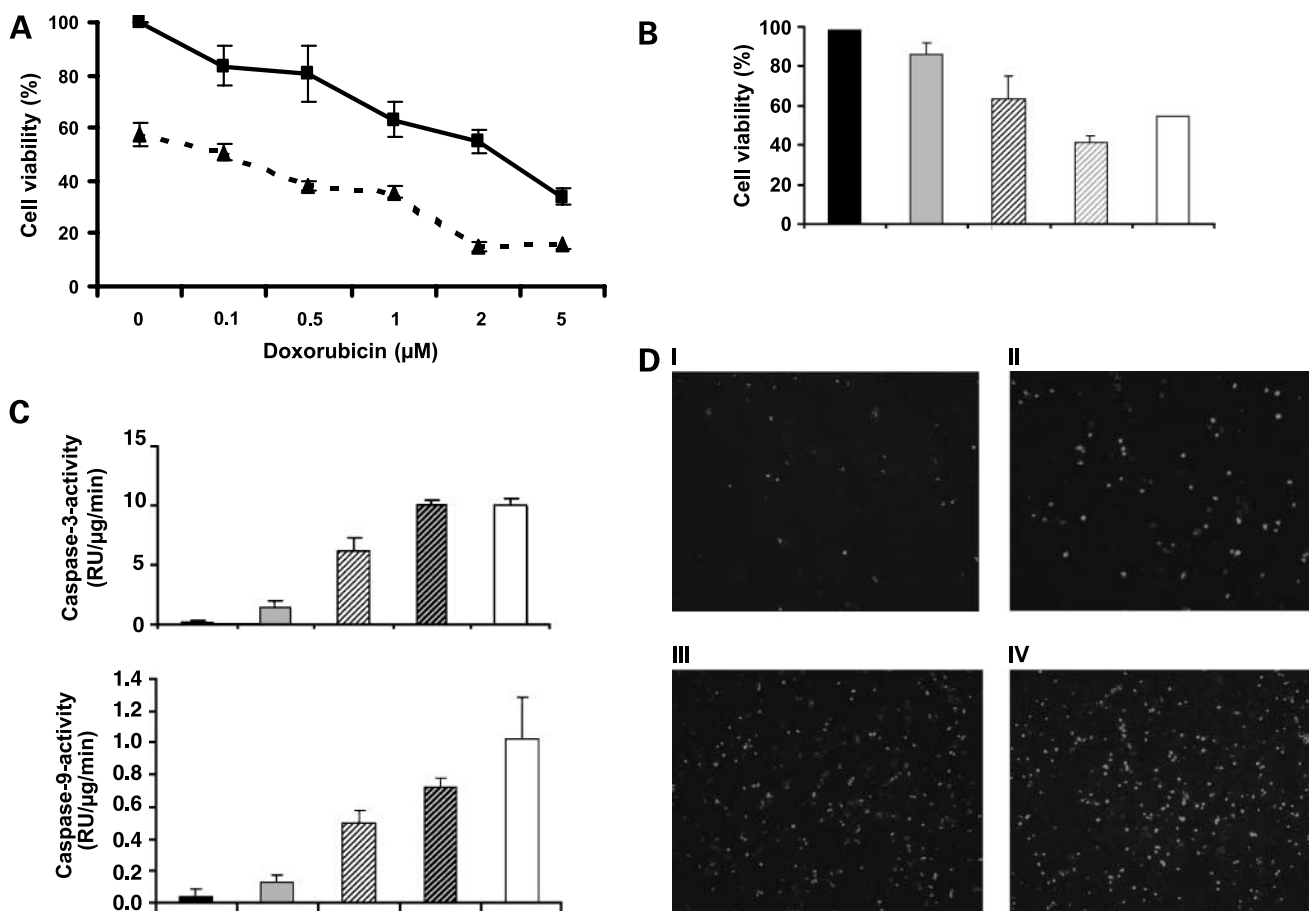


Figure 7. Doxorubicin enhanced the cytotoxic effect of LCL-30. **A**, MTT assay. Cells were incubated for 24 h with doxorubicin in combination with vehicle [0.05% (v/v) ethanol] or LCL-30 (5 μmol/L). *Points*, mean of duplicate determination of three independent experiments; *bars*, SD. *Black line*, vehicle; *dotted line*, LCL-30 (5 μmol/L). **B**, trypan blue exclusion test. Synergy was assessed by comparing predicted effect (*open column*) with observed effect (*gray striped column*) of cotreatment according to the fractional product method. *Columns*, mean of three independent experiments measured in duplicate; *bars*, SD. *Black column*, control; *gray column*, doxorubicin (1 μmol/L); *white striped column*, LCL-30 (5 μmol/L); *gray striped column*, LCL-30/doxorubicin (5 μmol/L/1 μmol/L); *white column*, predicted cell viability. **C**, activity of caspase-3 and caspase-9 was measured after 12 h of incubation using Ac-DEVD-AFC and Ac-LEHD-AFC, respectively. The activity is represented as relative units/μg protein/min. Actinomycin D/tumor necrosis factor-α served as positive control. The combination of LCL-30 with doxorubicin significantly induced higher caspase activity than either compound alone ($P = 0.03$). *Columns*, mean of three independent experiments; *bars*, SD. *Black column*, control; *gray column*, doxorubicin (1 μmol/L); *white striped column*, LCL-30 (5 μmol/L); *black striped column*, doxorubicin/LCL-30 (1 μmol/L/5 μmol/L); *white column*, actinomycin D/TNF-α. **D**, terminal deoxynucleotidyl transferase-mediated dUTP nick end labeling staining after 12 h of treatment. *I*, control; *II*, doxorubicin (1 μmol/L); *III*, LCL-30 (5 μmol/L); *IV*, LCL-30/doxorubicin (5 μmol/L/1 μmol/L). Representative of three independent experiments.

enhanced uptake of doxorubicin or an increase of endogenous ceramide levels.

A novel chemotherapeutic approach is based on cytotoxic molecules that directly target mitochondria of cancer cells, thereby circumventing upstream proapoptotic pathway that might be mutated or lacking. The mitochondrial membrane permeabilization is considered to be the point-of-no-return in the cell death program. The breakdown of $\Delta\psi_m$ results in the release of proapoptotic molecules, such as cytochrome *c*, from mitochondria into the cytosol, activating the cell death machinery. Several findings suggest that the composition and function of normal and cancer cells differ. These include a higher $\Delta\psi_m$, possibly modulation of expression of permeability transition pore complex components, enhanced rates of ATP generation through glycolysis rather than through oxidative phosphorylation (the Warburg effect), and a higher susceptibility to oxidative stress by a higher endogenous level of ROS (17–20, 39). There is strong evidence that mitochondria are one of the major targets of exogenous ceramides (40) rendering ceramides promising new drugs for cancer therapy.

Because natural, long-chain ceramides are not water-soluble and do not penetrate cellular membranes, synthetic short-chain ceramides (C_2 - and C_6 -ceramides) have been developed to study the biological behavior of ceramide. However, whether the effects of short-chain ceramides fully mimic those of naturally occurring long-chain ceramide species remains unclear. Short-chain ceramides also exhibit different partitioning and behavior in biomembranes (e.g., localization to the Golgi apparatus or the endoplasmic reticulum; refs. 41–43). Furthermore, many of the studies were done using isolated mitochondria. In the endoplasmic reticulum, C_2 -ceramide inhibits the biosynthesis of phosphatidylcholine and phosphatidylethanolamine (44, 45). The inhibition of phospholipid synthesis may block vesicular trafficking and may directly cause apoptosis (46). To circumvent these shortcomings, we developed a novel cationic long-chain (C_{16}) ceramide (LCL-30), directly targeting the negatively charged mitochondria and creating a tool to investigate the biological effects of naturally occurring long-chain ceramide species.

The cationic long-chain ceramide compound LCL-30 induced cell death in SW403 cancer cells. Analysis of the cellular ceramide pool revealed a decrease of the total endogenous ceramide concentration in LCL-30-treated cells, which is in sharp contrast to other reports using short-chain ceramides. For example, after administration of C_6 -ceramide, the endogenous ceramide pool was shown to increase in HepG2 in Chinese hamster ovary cells (47) and in lung adenocarcinoma A549 cells (48). Total ceramide and sphingosine levels also increased in Jurkat cells after treatment with C_2 -ceramide (49). This observation supports the concept that exogenous short- and long-chain ceramides differ in many aspects. Interestingly, the decrease of endogenous ceramide concentration in our study is explained by the selective reduction of the ceramide concentration in mitochondria because no change of the

ceramide pool was detected in the extramitochondrial (nuclei/plasma membranes) and cytosolic fractions, respectively. Moreover, only the most abundant ceramide species C_{16} and $C_{24:1}$ were affected, whereas the other ceramides (C_{14} , $C_{18:0}$, $C_{18:1}$, C_{20} , and C_{24}) remained unaffected in all of the three cellular fractions. The decline of the proapoptotic endogenous ceramides C_{16} and $C_{24:1}$ might be interpreted as a defense mechanism of the mitochondrion attacked by a long-chain ceramide. The lack of an increase in total ceramide level after long-chain ceramide administration is in line with recent data showing that apoptotic activity of soluble analogues of C_{16} -ceramide did not rely on endogenous ceramide elevation before cell death (50). Unlike ceramide analogues causing an increase in endogenous ceramide levels [e.g., short-chain ceramides, B13 (7)], the effects of the cationic long-chain ceramides may not be circumvented by activation of ceramide metabolism. Such an increased capacity to metabolize ceramides has been shown for cancer cells (34, 51) leading to resistance to radiation or chemotherapy. Thus, by bypassing ceramide metabolism, these novel compounds have an additional advantage in cancer therapeutics.

Ceramide can be metabolized by ceramidase producing the proapoptotic sphingosine, which in turn may be phosphorylated by sphingosine kinases to form S1P. To date, two isoforms of sphingosine kinases are known, SphK1 and SphK2. Conversely, S1P has been implicated as signaling molecule that antagonizes apoptotic cell death. The dynamic balance among ceramide, sphingosine, and S1P seems to determine survival of the cell.

S1P is a specific ligand of a family of five G-protein-coupled cell surface receptors ($S1P_{1-5}$). On stimulation, signaling cascades implicated in apoptosis, such as cytochrome *c* release from mitochondria, activation of caspases, and activation of the stress-activated protein kinase *c-Jun* NH₂-terminal kinase, may be inhibited (reviewed in ref. 32). This also holds true for ceramide-mediated apoptosis, which was reported to be suppressed by S1P (52).

We observed that LCL-30 induced a selective up-regulation of S1P in mitochondria of SW403 cells, whereas S1P levels in cytosol and the extramitochondrial cellular fraction remained unaltered. Along with the decrease of mitochondrial ceramide levels, the increase of S1P likewise implies a mitochondrial defense mechanism in response to mitochondriotoxic agents. The observed alterations of mitochondrial S1P allude to the presence of a mitochondrial sphingosine kinase, which is selectively activated on treatment with exogenous ceramides.

Doxorubicin is a cationic lipophilic molecule as LCL-30, which is suggested to accumulate in mitochondria. When SW403 cells were cotreated with LCL-30 and doxorubicin, we observed a synergistic effect on cell viability. This synergistic action was also evident in an overadditive increase of caspase-3 and caspase-9 activity and the number of cells with dissipated $\Delta\psi_m$, suggesting mitochondria to be a target of doxorubicin in SW403 cells. This phenomenon has also been recently described using short-chain pyridinium

ceramides and doxorubicin in HepG2 cells (53). However, in our hands, doxorubicin did not induce any alteration in endogenous ceramide levels in the cellular fractions analyzed (mitochondrial, cytosolic, and extramitochondrial). This is in contrast to several publications showing elevation of ceramide levels induced by anthracyclines (2, 34–38). Moreover, cotreatment of LCL-30 and doxorubicin did not result in an increase of mitochondrial S1P levels. These observations suggest that (a) the synergistic effect of doxorubicin and LCL-30 in SW403 cells is not founded on the level of sphingolipids and (b) the increase of S1P and the decrease of endogenous ceramide in mitochondria might be specifically related to the application of a mitochondrially targeted ceramide. However, further studies are needed to elucidate the precise mechanism of this drug synergism. Additionally, the exclusive mitochondrial alteration in sphingolipid levels has to be further explored using other mitochondriotoxic molecules.

There are some considerations that have to be taken into account while interpreting the results of this study. First, although LCL-30 was predominantly found in mitochondria, we cannot rule out the possibility that LCL-30 may also accumulate in other organelles, such as the endoplasmic reticulum and the Golgi, or might be gathered in microsomal membranes that tightly associate with mitochondria. However, there are no ultrastructural alterations of other organelles than mitochondria as identified in transmission electron microscopy. The destruction of mitochondrial architecture was the only pathologic finding, which suggests mitochondria to be the major target of cellular death executors induced by LCL-30. Second, the biochemical effects of LCL-30 have been extensively studied in only one cell line (human colon cancer cell line SW403). Different molecular pathways of cell death induction in other cancer cell lines cannot be excluded. However, LCL-30 was shown to induce cell death in a variety of other cancer cell lines (human colon carcinoma and hepatoma cell lines). Third, LCL-30 was not found to be toxic in freshly isolated hepatocytes. This finding supports the concept of selective toxicity of ceramides but does not answer the question of *in vivo* tolerability. Only animal studies, which are currently done by our group, may elucidate the role of LCL-30 or related compounds as a potential novel drug for cancer therapy.

In conclusion, we present a novel cationic long-chain pyridinium ceramide (LCL-30) causing apoptosis in a variety of cancer cells, including SW403 human colon cancer cells. In SW403, LCL-30 preferentially accumulated in mitochondria resulting in a selective decrease of the mitochondrial pool of endogenous ceramides. Moreover, we observed an increase of S1P in mitochondria, suggesting the presence of a mitochondrial sphingosine kinase. Alterations of mitochondrial sphingolipid levels might be interpreted as a regulated cellular defense mechanism against mitochondriotoxic drugs. Based on the numerous differences between mitochondria of normal and cancer cells, cationic long-chain pyridinium ceramides might be promising new drugs for cancer therapy by their mito-

chondrial preference. Furthermore, by the use of these novel ceramides, new insights might be gained into the function and regulation of mitochondrial sphingolipids. The efficacy and safety of LCL-30 is currently being tested in an animal model by our group.

References

- Pettus BJ, Chalfant CE, Hannun YA. Ceramide in apoptosis: an overview and current perspectives. *Biochim Biophys Acta* 2002;2–3: 114–25.
- Bose R, Verheij M, Haimovitz-Friedman A, Scotto K, Fuks Z, Kolesnick R. Ceramide synthase mediates daunorubicin-induced apoptosis: an alternative mechanism for generating death signals. *Cell* 1995;3:405–14.
- Senchenkov A, Litvak DA, Cabot MC. Targeting ceramide metabolism—a strategy for overcoming drug resistance. *J Natl Cancer Inst* 2001; 5:347–57.
- von Haefen C, Wieder T, Gillissen B, et al. Ceramide induces mitochondrial activation and apoptosis via a Bax-dependent pathway in human carcinoma cells. *Oncogene* 2002;25:4009–19.
- Jones BE, Lo CR, Srinivasan A, Valentino KL, Czaja MJ. Ceramide induces caspase-independent apoptosis in rat hepatocytes sensitized by inhibition of RNA synthesis. *Hepatology* 1999;1:215–22.
- Ping SE, Barrett GL. Ceramide can induce cell death in sensory neurons, whereas ceramide analogues and sphingosine promote survival. *J Neurosci Res* 1998;2:206–13.
- Selzner M, Bielawska A, Morse MA, et al. Induction of apoptotic cell death and prevention of tumor growth by ceramide analogues in metastatic human colon cancer. *Cancer Res* 2001;3:1233–40.
- Garcia-Ruiz C, Colell A, Mari M, Morales A, Fernandez-Checa JC. Direct effect of ceramide on the mitochondrial electron transport chain leads to generation of reactive oxygen species. Role of mitochondrial glutathione. *J Biol Chem* 1997;17:11369–77.
- Di Paola M, Cocco T, Lorusso M. Ceramide interaction with the respiratory chain of heart mitochondria. *Biochemistry* 2000;22:6660–8.
- Novgorodov SA, Szulc ZM, Luberto C, et al. Positively charged ceramide is a potent inducer of mitochondrial permeabilization. *J Biol Chem* 2005;16:16096–105.
- Ruvolo PP, Deng X, Ito T, Carr BK, May WS. Ceramide induces Bcl2 dephosphorylation via a mechanism involving mitochondrial PP2A. *J Biol Chem* 1999;29:20296–300.
- Bidere N, Lorenzo HK, Carmona S, et al. Cathepsin D triggers Bax activation, resulting in selective apoptosis-inducing factor (AIF) relocation in T lymphocytes entering the early commitment phase to apoptosis. *J Biol Chem* 2003;33:31401–11.
- Birbes H, El Bawab S, Hannun YA, Obeid LM. Selective hydrolysis of a mitochondrial pool of sphingomyelin induces apoptosis. *FASEB J* 2001; 14:2669–79.
- El Bawab S, Roddy P, Qian T, Bielawska A, Lemasters JJ, Hannun YA. Molecular cloning and characterization of a human mitochondrial ceramidase. *J Biol Chem* 2000;28:21508–13.
- Shimeno H, Soeda S, Sakamoto M, Kouchi T, Kowakame T, Kihara T. Partial purification and characterization of sphingosine *N*-acyltransferase (ceramide synthase) from bovine liver mitochondrion-rich fraction. *Lipids* 1998;6:601–5.
- Gudz TI, Tserng KY, Hoppel CL. Direct inhibition of mitochondrial respiratory chain complex III by cell-permeable ceramide. *J Biol Chem* 1997;39:24154–8.
- O’Gorman E, Beutner G, Dolder M, Koretsky AP, Brdiczka D, Wallimann T. The role of creatine kinase in inhibition of mitochondrial permeability transition. *FEBS Lett* 1997;2:253–7.
- Barath P, Albert-Fournier B, Luciakova K, Nelson BD. Characterization of a silencer element and purification of a silencer protein that negatively regulates the human adenine nucleotide translocator 2 promoter. *J Biol Chem* 1999;6:3378–84.
- Galiegue S, Jbilo O, Combes T, et al. Cloning and characterization of PRAX-1. A new protein that specifically interacts with the peripheral benzodiazepine receptor. *J Biol Chem* 1999;5:2938–52.
- Chen LB. Mitochondrial membrane potential in living cells. *Annu Rev Cell Biol* 1988;4:155–81.

21. Ghafourifar P, Klein SD, Schucht O, et al. Ceramide induces cytochrome *c* release from isolated mitochondria. Importance of mitochondrial redox state. *J Biol Chem* 1999;10:6080–4.
22. Castedo M, Hirsch T, Susin SA, et al. Sequential acquisition of mitochondrial and plasma membrane alterations during early lymphocyte apoptosis. *J Immunol* 1996;2:512–21.
23. Siskind LJ, Kolesnick RN, Colombini M. Ceramide channels increase the permeability of the mitochondrial outer membrane to small proteins. *J Biol Chem* 2002;30:26796–803.
24. Kong JY, Rabkin SW. Mitochondrial effects with ceramide-induced cardiac apoptosis are different from those of palmitate. *Arch Biochem Biophys* 2003;2:196–206.
25. Schwandner R, Wiegmann K, Bernardo K, Kreder D, Kronke M. TNF receptor death domain-associated proteins TRADD and FADD signal activation of acid sphingomyelinase. *J Biol Chem* 1998;10:5916–22.
26. Hayter HL, Pettus BJ, Ito F, Obeid LM, Hannun YA. TNF α -induced glutathione depletion lies downstream of cPLA(2) in L929 cells. *FEBS Lett* 2001;2:151–6.
27. Liu B, Andrieu-Abadie N, Levade T, Zhang P, Obeid LM, Hannun YA. Glutathione regulation of neutral sphingomyelinase in tumor necrosis factor- α -induced cell death. *J Biol Chem* 1998;18:11313–20.
28. Papucci L, Schiavone N, Witort E, et al. Coenzyme q10 prevents apoptosis by inhibiting mitochondrial depolarization independently of its free radical scavenging property. *J Biol Chem* 2003;30:28220–8.
29. Ling YH, Liebes L, Zou Y, Perez-Soler R. Reactive oxygen species generation and mitochondrial dysfunction in the apoptotic response to bortezomib, a novel proteasome inhibitor, in human H460 non-small cell lung cancer cells. *J Biol Chem* 2003;36:33714–23.
30. Muriel MP, Lambeng N, Darios F, et al. Mitochondrial free calcium levels (Rhod-2 fluorescence) and ultrastructural alterations in neuronally differentiated PC12 cells during ceramide-dependent cell death. *J Comp Neurol* 2000;2:297–315.
31. Wagenknecht B, Roth W, Gulbins E, Wolburg H, Weller M. C2-ceramide signaling in glioma cells: synergistic enhancement of CD95-mediated, caspase-dependent apoptosis. *Cell Death Differ* 2001;6:595–602.
32. Spiegel S, Milstien S. Sphingosine-1-phosphate: an enigmatic signalling lipid. *Nat Rev Mol Cell Biol* 2003;5:397–407.
33. Rebbaa A, Chou PM, Emran M, Mirkin BL. Doxorubicin-induced apoptosis in caspase-8-deficient neuroblastoma cells is mediated through direct action on mitochondria. *Cancer Chemother Pharmacol* 2001;6:423–8.
34. Itoh M, Kitano T, Watanabe M, et al. Possible role of ceramide as an indicator of chemoresistance: decrease of the ceramide content via activation of glucosylceramide synthase and sphingomyelin synthase in chemoresistant leukemia. *Clin Cancer Res* 2003;1:415–23.
35. Andrieu-Abadie N, Jaffrezou JP, Hatem S, Laurent G, Levade T, Mercaider JJ. L-Carnitine prevents doxorubicin-induced apoptosis of cardiac myocytes: role of inhibition of ceramide generation. *FASEB J* 1999;12:1501–10.
36. Delpy E, Hatem SN, Andrieu N, et al. Doxorubicin induces slow ceramide accumulation and late apoptosis in cultured adult rat ventricular myocytes. *Cardiovasc Res* 1999;2:398–407.
37. Jaffrezou JP, Levade T, Bettaieb A, et al. Daunorubicin-induced apoptosis: triggering of ceramide generation through sphingomyelin hydrolysis. *EMBO J* 1996;10:2417–24.
38. Lucci A, Han TY, Liu YY, Giuliano AE, Cabot MC. Modification of ceramide metabolism increases cancer cell sensitivity to cytotoxics. *Int J Oncol* 1999;3:541–6.
39. Pelicano H, Feng L, Zhou Y, et al. Inhibition of mitochondrial respiration: a novel strategy to enhance drug-induced apoptosis in human leukemia cells by an ROS-mediated mechanism. *J Biol Chem* 2003;278:37832–9.
40. Radin NS. Killing tumours by ceramide-induced apoptosis: a critique of available drugs. *Biochem J* 2003 Pt 2;243–56.
41. van Blitterswijk WJ, van der Luit AH, Veldman RJ, Verheij M, Borst J. Ceramide: second messenger or modulator of membrane structure and dynamics? *Biochem J* 2003 Pt 2;199–211.
42. Ardail D, Popa I, Bodennec J, Famy C, Louisot P, Portoukalian J. Subcellular distribution and metabolic fate of exogenous ceramides taken up by HL-60 cells. *Biochim Biophys Acta* 2002;3:305–10.
43. Pagano RE, Martin OC, Kang HC, Haugland RP. A novel fluorescent ceramide analogue for studying membrane traffic in animal cells: accumulation at the Golgi apparatus results in altered spectral properties of the sphingolipid precursor. *J Cell Biol* 1991;6:1267–79.
44. Allan D. Lipid metabolic changes caused by short-chain ceramides and the connection with apoptosis. *Biochem J* 2000;345 Pt3:603–10.
45. Bladergroen BA, Bussiere M, Klein W, Geelen MJ, Van Golde LM, Houweling M. Inhibition of phosphatidylcholine and phosphatidylethanolamine biosynthesis in rat-2 fibroblasts by cell-permeable ceramides. *Eur J Biochem* 1999;1:152–60.
46. McMaster CR. Lipid metabolism and vesicle trafficking: more than just greasing the transport machinery. *Biochem Cell Biol* 2001;6:681–92.
47. Vieu C, Terce F, Chevy F, et al. Coupled assay of sphingomyelin and ceramide molecular species by gas liquid chromatography. *J Lipid Res* 2002;3:510–22.
48. Ogretmen B, Pettus BJ, Rossi MJ, et al. Biochemical mechanisms of the generation of endogenous long chain ceramide in response to exogenous short chain ceramide in the A549 human lung adenocarcinoma cell line. Role for endogenous ceramide in mediating the action of exogenous ceramide. *J Biol Chem* 2002;15:12960–9.
49. Cuvillier O, Edsall L, Spiegel S. Involvement of sphingosine in mitochondria-dependent Fas-induced apoptosis of type II Jurkat T cells. *J Biol Chem* 2000;21:15691–700.
50. Bieberich E, Hu B, Silva J, et al. Synthesis and characterization of novel ceramide analogs for induction of apoptosis in human cancer cells. *Cancer Lett* 2002;1:55–64.
51. Liu YY, Han TY, Giuliano AE, Cabot MC. Ceramide glycosylation potentiates cellular multidrug resistance. *FASEB J* 2001;3:719–30.
52. Cuvillier O, Pirianov G, Kleuser B, et al. Suppression of ceramide-mediated programmed cell death by sphingosine-1-phosphate. *Nature* 1996;6585:800–3.
53. Rossi MJ, Sundararaj K, Koybasi S, et al. Inhibition of growth and telomerase activity by novel cationic ceramide analogs with high solubility in human head and neck squamous cell carcinoma cells. *Otolaryngol Head Neck Surg* 2005;1:55–62.